CMT Ceramics in Modern Technologies
Techna Group srl

Rheological Evaluation of Phosphatic Porcelain using Squeeze Flow Technique

K. Ino[a], F.A. Cardoso[b], G.A. Valencia[b], R.G. Pileggi[b], A.L. da Silva[a], L.B. Caliman[a]*, D. Gouvêa[a]
[a]Department of Metallurgical and Materials Engineering, Polytechnic School, University of São Paulo (USP), São Paulo - SP, Brazil; [b]Department of Civil Construction Engineering, Polytechnic School, University of São Paulo (USP), São Paulo - SP, Brazil

Phosphatic porcelain (PP), commonly known as bone china, constitutes approximately 50 wt% bone ash, 25 wt% kaolin, and 25 wt% feldspar, and its primary characteristics are high translucency and a high impact resistance. However, the low plasticity of these ceramic raw materials makes its moulding difficult owing to the plastic deformation due to the throwing wheel. Plasticizers or plasticity-promoting additives, such as sodium bentonite and methyl hydroxyethyl cellulose, modify the rheological behavior to pseudoplastic with a yield stress. Ceramic raw materials with plasticizers were prepared and characterized using helium pycnometry density, X-ray fluorescence, X-ray diffraction, and particle size distribution. In addition, characterization analysis was performed in commercial porcelain P905 for comparison purposes. The squeeze flow technique (compression of a cylindrical sample between two parallel plates) was employed to assess and compare the rheological behavior of the PP compositions with and without additives with the behavior of the commercial material. Results show that the addition of 4 wt% bentonite in the PP introduced a plasticity similar to that of the commercial porcelain, easing the shaping process using a throwing wheel. Plasticity index (PI) from the Atterberg test is useful; however, it is not sufficiently detailed to predict conformation performance of the ceramic raw materials in the throwing wheel as per the rheological information provided by the squeeze flow test.

Keywords: Phosphatic porcelain, Plasticity, Throwing wheel, Bentonite, Squeeze flow.

1. Introduction

Phosphatic porcelain (PP), or bone china, is a ceramic scarcely used or fabricated in Latin America. There is no industrial-scale production in Brazil, despite the abundantly available renewable raw material, the bovine bones [1]. The 2019 Brazilian annual production of bovine bone is estimated to be approximately 8 million tons (2.01 million tons in the second trimester) [2]. The traditional composition of PP is 50 wt% bone ash, 25 wt% kaolin, and 25 wt% feldspar, for which the non-plastic (bone ash and feldspar) fraction corresponds to 75 wt% [3-4]. Nevertheless, at low scales, such as the artistic ceramic, PP has a great potential due to its superior whiteness, translucency, and impact resistance compared to those of the traditional ceramics. Regardless of these advantages, PP mass is inferiorly plastic, which narrows down the possible conformation methods. Therefore, slip casting is the traditional conformation method used for PPs.

Ceramic conformation through plastic deformation is highly productive compared to the slip casting method and can be performed both manually and automatically. The throwing wheel, among the others plastic conformation techniques, is widely used in both industry and artisanal ceramic production, allowing high speed and productivity in the production of ceramics pieces [5]. However, ceramic pastes with reduced plasticity, such as PP, are not suitable for this type of conformation, and thus, it is necessary to increase their plasticity to adapt the ceramic paste to the conformation method.

High resistance to flow at high tensions and low resistance to flow at low tensions in the ceramic paste are the inverse effects of plasticity. This is the result of physical interaction between the particles, where the collisions become more frequent, and friction becomes more intense as the shear rate increases. Consequently, the viscosity increases significantly, possibly causing the rupture of the ceramic paste under deformation. On the contrary, plastic ceramic pastes are agglomerated and are present as gel structures in which the particles are attracted by van der Waals forces, resulting in structures with weak chemical bonds that are easily broken at low shear rates. Consequently, the viscosity decreases, producing a pseudoplastic and a thixotropic behavior [6]. In that case, the conformation using a throwing wheel is favored, allowing the execution of ceramic pieces with high uniformity, and is capable of maintaining its final form and not collapsing under its own weight once the deformation tension is withdrawn.

The increase in plasticity in the ceramic pastes can be achieved by adding natural plasticizer agents, which are the additives that promote plasticity, such as bentonites, which are plastic clays mainly composed of montmorillonite of the smectite group [7]. The main effect of montmorillonite presence is the destabilization of the particle dispersion condition through its capacity of gelling, which changes the rheological behavior of the clay. Depending on the medium pH, gelling can form different structures. In acid mediums, the structure of a card-house is favored due to

* *Corresponding author*
E-mail address: lorenabatistacaliman@gmail.com

https://doi.org/10.29272/cmt.2019.0016
Received June 18, 2019; Received in revised form December 3, 2019; Accepted December 4, 2019

interaction between the bigger and the smaller faces, face to edge (FE); in the basic medium, a structure named band-type is formed due to the interaction between the bigger faces, face to face (FF) [8-9]. Another characteristic is the interlamellar swelling and the water retention [10]. This amount of water retained in the structure has a lubricating effect between the particles when subjected to shear.

Additives are substances added in small quantities to alter or improve some characteristics of a material, such as a change in the rheological behavior of highly concentrated suspensions. The desired effects of a plasticizer additive in a ceramic suspension and its characteristics are the increase in plasticity, low or no reactivity with constituent raw materials of the ceramic paste, complete decomposition without trace during sintering, and being economically suitable. Suitable plasticizers for ceramic pastes are the additives based on cellulose ether. These additives are widely used in cement-based materials as water retainers and as viscosity modifiers, aiming to avoid phase separation in self-compacting, pumped, and sprayed mortar, and concrete formulations. The most commonly used cellulose ethers are methyl hydroxyethyl cellulose (MHEC) and methyl hydroxypropyl cellulose (MHPC) [11].

The ideal amount of water in the ceramic pastes for throwing wheel conformation varies according to the mineral composition, the particle size distribution, the interfacial forces, and the additives [12]. The amount of water in the plastic ceramic pastes has a direct influence on the yield stress. For low amounts of water, yield stress increases and presents a little deformation before rupturing. On the contrary, a high amount of water allows the ceramic body to deform further without rupturing under a low yield stress [13]. Indirect methods of plasticity measurement were developed, correlating the amount of water with the plasticity, such as the Pfefferkorn method, the cone penetration, and the Atterberg method. The Atterberg method defines that the plasticity index can be determined by the difference between the liquid limit (LL) and the plastic limit (PL), and each one corresponds to a different amount of water (LL > PL) associated to the opposite consistency levels.

Rheological evaluation of highly consistent pastes using the rotational rheometers is difficult because of the high levels of torque (stress) involved, the possibility of slip between the shear element, the tested material, and the plasticity of the pastes that can cause loss of contact during the test [14–17]. Alternatively, the squeeze-flow method allows the rheological evaluation of several materials, including the ceramic pastes, [15, 18, 19] in a wide range of consistency for flow conditions with geometrical confinement, with different deformation rates and degrees through the compression of a sample between two parallel plates [10–11]. The squeeze-flow method presents some characteristics that justify its successful application for cement-based materials [14, 16, 20, 21] that can be applied to the ceramic pastes conformed in a throwing wheel. These are: (i) the technique can be implemented in the universal machines usually available in universities, industries, and research centers with ease; (ii) the progressive geometrical confinement and the types of strain and stress generated (shear and/or elongation) are similar to the phenomena that happen in the paste between the operator's fingers during the manual conformation, including the occurrence of liquid-solid phase separation; (iii) the technique is quantitative and sensitive to the material's characteristics, and with some considerations allows for the determination of rheological parameters [14–17].

One method to analyze the curves generated by the squeeze-flow test is to identify the three possible behavior stages. The first step is to identify the material's elastic behavior related to the yield stress with small deformation, followed by the plastic stage or the viscous flow stage without any significant increase in the load or stress to continue the material's deformation, and last, the strain hardening stage, caused by the intense increase in the load or the stress [14, 16, 20], according to Fig. 1 [14]. In the last stage, molding and finishing of the ceramic piece difficulties due to the high stresses involved owing to the friction forces that are predominant in this situation.

This study proposes the influence of bentonite or MHEC in the rheological behavior of PP pastes using the squeeze-flow method. In addition, the behavior of a commercial porcelain ceramic paste for throwing wheel conformation is determined and used as a reference. The results were compared with the ones generated by the Atterberg plasticity test [12, 22], in addition to the manual conformation tests of the throwing wheel.

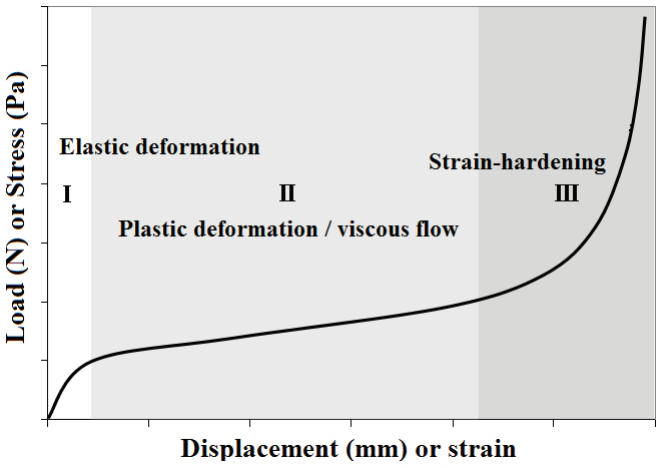

Figure 1. Typical displacement-controlled squeeze-flow profile; I shows elastic deformation, II shows viscous flow and/or plastic deformation, and III shows strain-hardening stage [14].

2. Experimental

2.1. Materials

The bovine bone ash used was generated as follows: (i) the bovine bones were washed and then cleaned in an autoclave to eliminate the organic matter (blood and fat); (ii) calcination in a furnace (ML 1300/40, Fortelab) at a heating rate of 1 °C/min up to 300 °C and then at 4 °C/min up to 1000 °C with a holding time of 240 min using air flow injection during the whole calcination period; (iv) drying in a stove at 110 °C for 24 h [23].

PP was prepared at a laboratory scale (500 g) with composition as 50 wt% bovine bone ash (obtained as previously), 25 wt% of kaolin (mesh #200 washed from Rio do Rastro mining, SP-Brazil) and 25 wt% of potassium feldspar (mesh #200 from Marc Mineração mining, Ponta Grossa, PR-Brazil). The mixture was processed for 24 h in a ball mill using alumina milling elements and 500 ml of deionized water. After drying in a stove at 110 °C for 24 h [23, 24], the material was deagglomerated manually in a mortar and sieved using a 0.42 mm open mesh.

Sodic bentonite from the Patagônia region of Argentina, constituting of montmorillonite with a loss on ignition (LoI) of 14.6 wt%, was added to the PP ceramic paste (before the milling step) with either 2 wt% or 4 wt% of the dry material. Samples were labeled PP2% B and PP4% B, respectively. The cellulose additive, a cellulose ether-type methyl hydroxyethyl cellulose (MHEC Combizell LH 40M, Ashland Inc.), was added to the mixture before milling in 0.5 wt% and 1 wt%. Samples were labeled PP0.5% MHEC and PP1% MHEC, respectively.

A commercial high-temperature porcelain (P905) for cone firing 10–1300 °C fabricated in Canada and commercialized by PSH Brasil Ltda for manual conformations, sculptures, and throwing wheel was used as a reference [25].

2.2. Methods

The densities of the powders were obtained using a Micrometrics AccuPyc II model 1340 gas pycnometer with a 1.0 cm^3 chamber and 10 cycles of 50 purges. Particle size distribution using laser diffraction was performed in a dispersion of the powder in alcohol using a Helos/SUCELL, Sympatec GmbH.

The chemical composition of the materials was determined by X-ray fluorescence (XRF) using a S8 Tiger, Bruker, dosing the element between fluorine and uranium. The mineral structure was determined by X-ray diffraction (DRX) using an X'Pert PRO, PANalytical with an X'Celerator detector, Cu tube (45 mA 40 kV energy, 2 θ range of 2.5° ~ 70° and 0.02° steps per 100 s.

Electrophoretic dynamic mobility as a function of the pH of the aqueous dispersion of PP with and without additives was assessed in a ESA 9800 Zeta Potential Analyzer, Matec with a total capacity of 230 ml, where 5 v% of the sample (11.5 ml) was dispersed in 218.5 ml of deionized water prepared 24 h prior to the test.

Plasticity tests were performed as per the Atterberg method to determine the water content in the ceramic pastes, the plastic limit (PL) according to the Brazilian standard NBR7180 (the minimum amount of water to roll clay in a 150 mm long cylinder with diameter of 3–4 mm), and the liquid limit (LL) (the amount of water where the clay starts to flow as a liquid). The test was performed in a Casagrande apparatus, regulated by the Brazilian Standard NBR6459. The plasticity index (PI) is the difference between LL and PL [12].

A throwing wheel RK-3D model, Shimpo, with a rotation capacity of 250 rpm was used to fabricate the ceramic pieces. Water was added to the dry ceramic pastes 24 h prior to the tests in a hermetic recipient for homogenization. The test molds the paste in a cylindrical form maintaining a uniform wall at a rotation speed of 180 rpm. Each test was performed with a 150 g sample.

Presently there is no mathematic model that describes the behavior of ceramic pastes in an electrical throwing wheel, thus, the analysis in this study will be a comparison between the prepared ceramic paste and the reference ceramic paste (Porcelain 905 for cone firing 10–1300 °C). This sample has been referred as P905.

Rheometry analysis using the squeeze flow method was performed using a 5569 model, Instron universal testing machine with capacity of 50 kN, a load cell of 1 kN (Fig. 2), a 200 mm diameter inferior steel plate, and a 101 mm diameter stainless steel top plate [14,20]. Both plates had smooth surfaces. The cylindrical samples were molded with 50 mm diameter and 10 mm height. The height was adjusted in a template of 10 mm thick wood fillets and cut with a 50 mm diameter stainless steel cutter as shown in Fig. 3. The constant volume configuration (Fig. 4) was chosen to decrease the edge effects. Each sample was subjected to two different displacement speeds of 0.1 mm/s and 5.0 mm/s, considering the order of magnitude in which the phenomena occur in practical situations. End of the test was determined with a 9 mm maximum displacement or a 1 kN maximum normal force, whichever was reached first [14, 20, 21]. P905 (reference) was tested with three different amounts of water, 31 v%, 39 v%, and 46 v%, respectively, and the PPs with 45 v% in water.

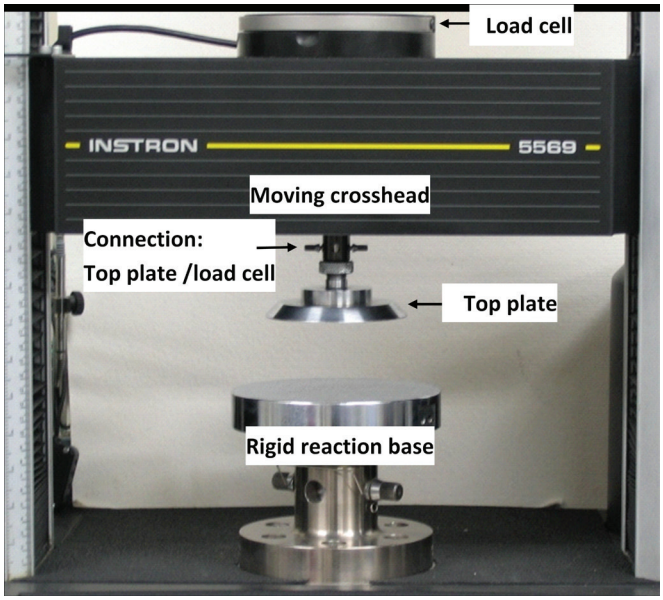

Figure 2. Testing machine, INSTRON (Model 5569, Capacity 50 kN, Load cell 1kN).

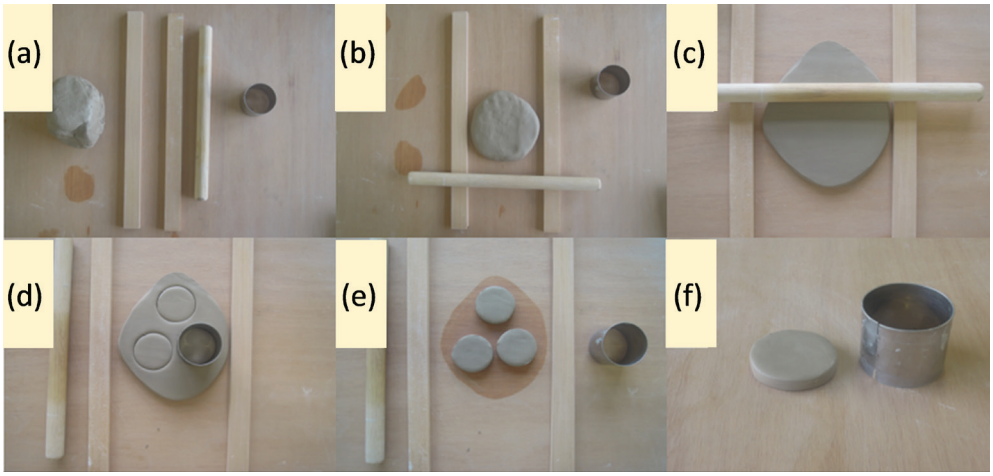

Figure 3. Method of sample preparation for squeeze-flow tests: (a) ceramic paste, two wood fillets of thickness 10 mm, a wooden roller, and a stainless steel cutter of diameter 50 mm; (b) positioning the ceramic paste between fillets; (c) through roller adjust the paste's height equal to the thickness of fillets; (d) cut samples through stainless steel cutter; (e) removing paste around samples; (f) sample measuring 50 mm diameter and 10 mm height.

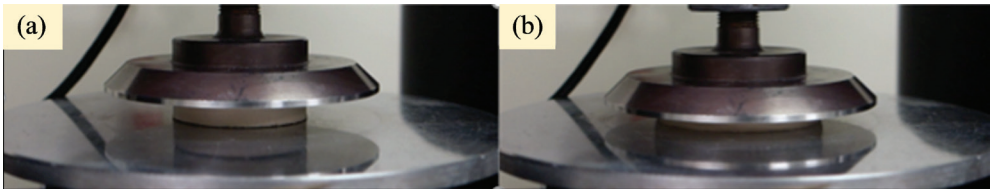

Figure 4. Constant volume squeeze-flow setup: (a) beginning of test, sample diameter 50 mm, height 10 mm, (b) end of test.

3. Results and Discussion

3.1. Chemical and mineralogical evaluation

Commercial porcelain, PP without additives and raw materials chemical compositions determined by XRF showed that the amount of iron oxide (Fe_2O_3) (< 2.5 wt%) and titanium oxide (TiO_2) (<0.5 wt%) are suitable for the aimed ceramic formulation. This information is relevant because a white ceramic is intended and the presence of these oxides leads to different colors formations (Table 1). The identified quantities of calcium oxide, CaO, (31.5 wt%) and phosphorus pentoxide, P_2O_5, (21.7 wt%) are decomposed from hydroxyapatite ($Ca_{10}(PO_4)_6(OH)_2$), major mineral constituent of bones, as it can be observed in Fig. 5. The other identified mineral constituents in the reference ceramic paste are kaolinite, albite, and quartz, commonly found in ceramic pastes. The phase analysis (Fig. 5) indicated the presence of montmorillonite in the sodic bentonite, besides the presence of gibbsite and quartz.

Table 1. Chemical composition analysis by XRF of ceramic pastes and raw materials.

Raw materials	Al_2O_3	SiO_2	Na_2O	K_2O	CaO	MgO	P_2O_5	Fe_2O_3	TiO_2	LoI
P905	22.8	64.8	0.51	2.37	0.31	0.93	0.19	0.45	0.11	6.89
PP without additives	12.5	23.5	1.10	3.26	31.5	0.55	21.7	0.26	0.38	5.25
Bone ash	0.14	0.17	0.75	0.05	60.6	0.83	35.3	<0.001	<0.001	1.86
Potassium Feldspar	19.4	65.8	3.23	10.3	<0.10	<0.10	-	0.20	<0.10	0.89
Rio do Rastro kaolin	38.4	46.8	<0.10	0.62	<0.10	<0.10	-	0.35	<0.10	15.1
Sodic Bentonite	15.0	49.5	2.79	0.24	3.35	5.14	6.04	2.35	0.19	14.6

3.2. Physical characteristics

Helium pycnometry density measurements indicate that ceramic pastes densities are approximately 2.5 g/cm³ for P905, 2.8 g/cm³ for PP, and 2.4 g/cm³ for the sodic bentonite additive.

The particle size distribution of P905 lies in the range of 0.2~100 μm, while PP presented a narrower range of 0.2~50 μm. The PP formulation with 4 wt% of bentonite presents particle size distribution in the same range as the pure PP, however with a smaller peak in the range of 2~10 μm, and a higher peak between 0.5 μm and 2 μm. This is attributed to the fact that pure bentonite was measured in the laser granulometer as received. However, because of the PP4% B formulation, bentonite was mixed with other raw materials prior to the milling process, as described in the Experimental Setup. Therefore, the bentonite present in PP4% B is finer than the pure raw material.

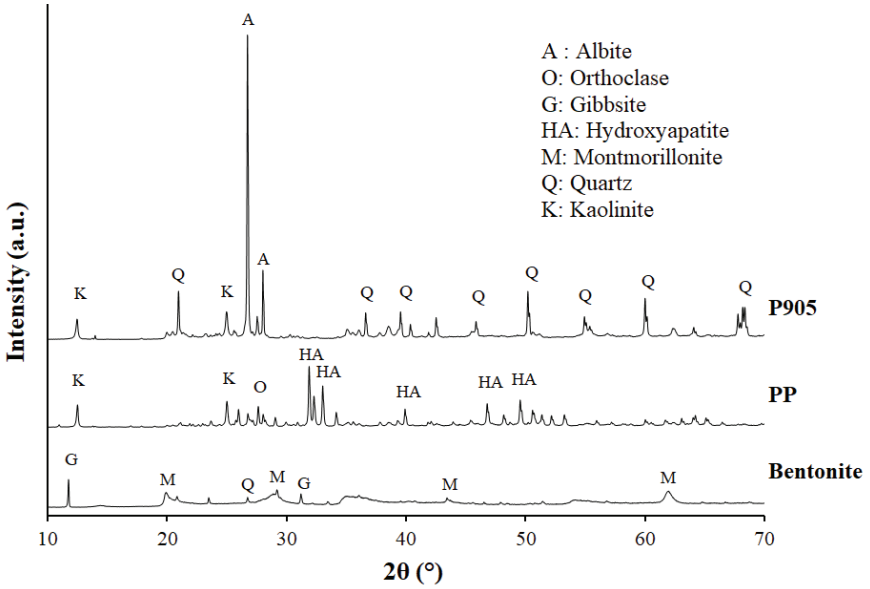

Figure 5. Phase analysis using XRD, P905, PP, and bentonite.

3.3. Atterberg's PI

PI results shown in Table 2 indicate that among all the tested ceramic pastes, P905 had the highest PI at 21%, meanwhile PP had a PI at 10%. With the addition of 2 wt% of bentonite, the PP2% B sample's PI changed to 14%, which was a 40% increase compared to that of the paste without the plasticity promoter additive. With 4 wt% of bentonite, the PP4% B's PI was 17%, which meant an increase of approximately 70%. The addition of 1 wt% of the organic additive MHEC increased the PP1% MHEC sample's PI to 16%. Both additives have the common characteristic of water retention in the system. Therefore, these additives added in adequate amounts increase the LL of the porcelain, allowing an addition of water before flowing as a liquid. The PL of PPs did not change in a significant way with the presence of additives; LL values were the most affected.

3.4. Dynamic electrophoretic mobility

The additive effects in PP can be analyzed according to the dynamic electrophoretic mobility presented in Table 3. The addition of 2 wt% of bentonite in the PP did not modify the pH values and conductivity. Nevertheless, when added at 4 wt%, the mobility was altered, increasing towards zero. As no other changes in either pH or conductivity were observed despite the decrease in the electrophoretic mobility, it can be inferred that this decrease might be associated to the interactions between

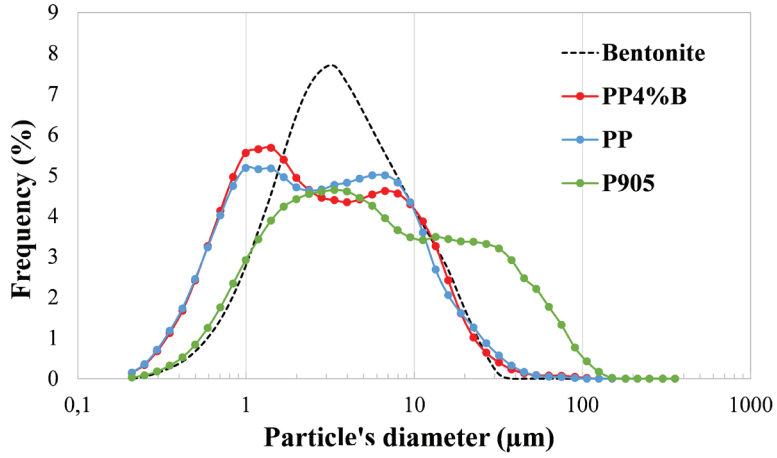

Figure 6. Particle size distribution of P905, PP, PP4% B, and bentonite.

Table 2. Porcelains PI in percentage by weight determined using the Atterberg limit test.

Samples		wt% of H_20			v% of H_20	
		PL	LL	PI	PL	LL
	P905	18	39	21	31	49
	PP	23	33	10	40	48
PP + additive	PP2% B	24	38	14	40	52
	PP4% B	23	40	17	38	53
	PP0.5% MHEC	23	33	10	39	48
	PP1% MHEC	23	39	16	39	52

Table 3. Dynamic electrophoretic mobility of PP with and without additives (T = 25 °C).

Composition	ESA (mPa*M/V)	pH	Conductivity (μS/cm)
PP	-1.691	10.8	1117.2
PP2%B	-1.618	10.8	1121.4
PP4%B	-0.264	10.7	1129.7
PP0.5% MHEC	-1.439	9.1	1363.7
PP1% MHEC	-0.826	9.1	1568.8

Table 4. Cylinder's dimension at the throwing wheel test of the three P905 samples.

Dimension	Porcelain n.1		Porcelain n.2		Porcelain n.3	
	Beginning (mm)	End (mm)	Beginning (mm)	End (mm)	Beginning (mm)	End (mm)
External diameter	77	67	74	64	77	66
Internal diameter	45	56	40	53	44	55
Height	21	45	20	45	19	47
Wall thickness	16	6	17	6	17	6

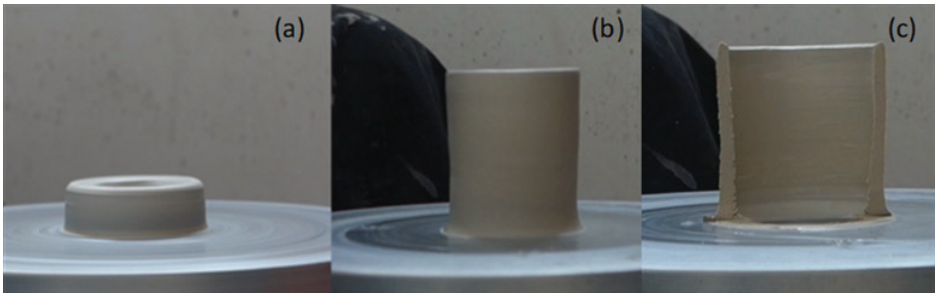

Figure 7. P905 cylinder sample: (a) at the beginning, (b) at the end, (c) uniform P905 wall thickness after rising in the cylindrical format on an electric throwing wheel.

the particles of the PP suspension and bentonite particles. The interaction between the particles favors the decrease in the electrophoretic mobility by increasing the total weight of the moving units. In a basic pH, montmorillonite is charged negatively, in both major and minor faces. Therefore, the colloidal particles are attracted to each other due to Van der Waals bonds, thus preferentially forming agglomerates of type FF (major faces) and reducing mobility because of the increase in the agglomerates' weight and volume.

The decrease in mobility with the presence of the additive MHEC can be due to the repulsion made by superficial adsorption of polymers of the ether cellulose functioning as a physical barrier (steric stabilization), thereby decreasing the system mobility. The variation of pH and conductivity may be caused by the solubility of MHEC in water as well as by the viscosity change of the aqueous medium.

3.5. Throwing wheel practical tests

The throwing wheel tests were performed taking into account the PI for P905, PP, PP4% B, and PP1% MHEC compositions. To verify the reproducibility of the process of raising the paste in a cylindrical format, three samples of P905 were used (Table 4 and Fig. 7). Despite small variations in the external and internal diameters among the samples, the final wall thickness of the three tests was the same (~ 6 mm) and displayed uniformity (Fig. 7). The average conformation speed in the reduction of the wall thickness (squeezing the paste between the fingers) was 1.4 mm/s. The behavior of the paste was adequate for the type of conformation applied.

For the paste with a low plasticity, like PP, it was not possible to form a uniform piece in the throwing wheel. Irregularities were formed on the wall during the process, and consequently, the body collapsed (Fig. 8a). Addition of 1% MHEC improved the paste consistency due to the modification of the water viscosity inside the system, increasing lubrication among the particles. Thus, it was possible to form a uniform piece; however, the cylinder deformed under its own weight at the end of the conformation. This suggests that the paste presented a lower yield stress, which is one of the effects of the cellulose ethers when added to suspensions [26]. For cementitious suspensions however, it only occurs for higher dosages, due to the intense agglomeration state in this kind of system. The addition of 4% bentonite in PP allowed the formation of the piece in a manner similar to the P905. Body deformation was not observed after the test, which indicates that the presence of bentonite modified the rheological behavior (Fig. 8). Thus, the shape of the piece was maintained after conformation due to the plasticity character provided by the bentonite.

3.6. Squeeze-flow

During the conformation practical tests of the cylindrical piece on the throwing wheel, the estimated average speed of wall thickness reduction was 1.4 mm/s. Therefore, squeeze-flow tests were performed at 0.1 and 5.0 mm/s, which comprehend the estimated practical value.

P905 was tested in the squeeze flow at three different water contents of 31 v% (plastic limit), 39 v% (ideal water content for conformation in the throwing wheel), and 46 v% (close to the liquid limit) (Fig. 9). Samples were labeled as P905_31%, P905_39%, and P905_46%, respectively. The 39 v% water content represents the initial amount of water when the paste was purchased from the supplier and presented the ideal behavior for conformation in the throwing wheel. Therefore, it was adopted as the ideal water content.

According to Fig. 9, P905_31% presented a rapid stress increase at the beginning, which is characteristic of the strain hardening stage. Although those curves have a high slope, they do not

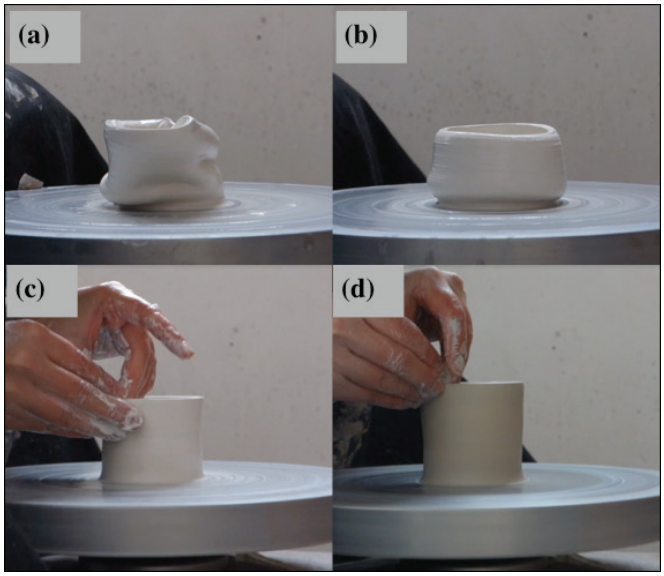

Figure 8. Porcelains on the throwing wheel test (a) PP without additive, (b) 1% MHEC, (c) 4 % bentonite, and (d) P905.

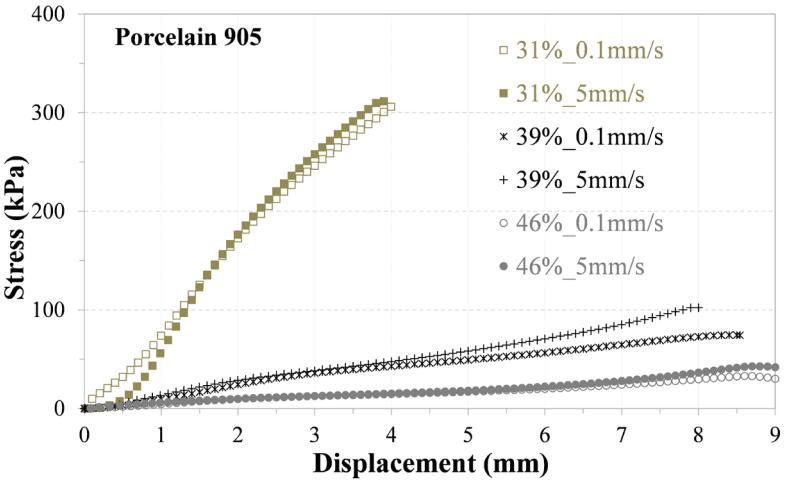

Figure 9. Squeeze flow results for P905 with three water contents (31 v%, 39 v%, 46 v%) tested at two displacement rates of 0.1 mm/s and 5.0 mm/s; stress values calculated considering area variation for constant volume deformation of an incompressible fluid.

present the expressive non-linear increase typical of this stage [14, 16, 20]. Probably, this is a reflex of the lubrication capacity of the clay present in the porcelain, even with a higher coefficient of friction due to the low water content used in this case. Considering the results from Table 2, the PL of the P905 is 31 v%, which means that the amount of water in the paste is still not enough to decrease the friction among the particles during the flow effectively, indicating a state of low plasticity. Increasing the water content led to a significant reduction in the stress required for deformation of the paste. However, it still reaches greater maximum deformations, being the curves characterized by the stage of plastic deformation. For all water contents, the curves obtained at different speeds did not present significant differences between them. This indicates that in this range of displacement rate, the behavior of this material does not show evidence of phase separation (solid-liquid) that can be induced during squeeze-flow [16, 19, 20].

For PP made in the laboratory, the initial amount of water was defined as 45 v%, which is above the PL of the Atterberg test (Table 2). The squeeze-flow curves of the PP without additive (Fig. 10) showed strain hardening for low displacements, such as P905_31% curves, indicating a paste with lower plasticity as indicated by the low PI. However, unlike P905_31%, in the PP, the third stage was manifested with usual characteristics that meant an expressive and a progressive non-linear stress increase. This behavior is associated to the granular response of a structure with higher friction levels due to high solid contents, phase separation (which increases the solid concentration in the central region), or even the compression of one or two particle layers as in the final stages of the mortar tests [16, 20]. Here, the phase separation is the predominant factor in the PP as the quantification of water content (dried at 110 °C for 24 h) in the central and peripheral regions after the squeeze-flow test indicated values of relative segregation of 5% for PP compared to 1% for the other ceramic pastes. Therefore, the lack of plasticity of PP is partly due to the tendency of phase separation and partly due to its own composition, which is formed of approximately 75 wt% non-plastic material and 25 wt% kaolin, which is known to have a lower plasticity than other clays.

Additives were employed in the PP paste aiming changes in the rheological behavior and the squeeze-flow results of the modified PP pastes are shown in Fig. 10. The PP2% B showed a behavior far from the reference paste. However, the benefits of bentonite were visible as it changed the intensity of the inversion to the strain hardening stage, reducing stress and resulting in greater final displacements (Fig. 10a). Nevertheless, with the addition of 4% bentonite, the PP did not show strain hardening behavior. On the contrary, it gained plasticity, as shown in the curve profile and in the final displacement, which was close to the reference commercial porcelain (P905). The montmorillonite clay present in the bentonite, above a certain amount destabilizes the dispersion behavior of the PP, owing to its gelation capacity where the water retained in the structure has a lubricating effect between the particles when subjected to shearing, avoiding phase separation (liquid-solid), and increasing the paste deformation capacity. In addition, the montmorillonite typically presents lamellae of approximately 1 nm in its structure with a high capacity of water retention between them, which can be oriented when subjected to shear and induce shear thinning effect. This favors the system plasticity especially at alkaline pH with face-to-face structure [8–10].

The pastes with the addition of MHEC (Fig. 10b) showed improvement characterized by greater final displacements than PP, especially for 0.1 mm/s. Because they are water-retentive polymer additives, they mainly modify the aqueous phase of the paste, increasing the water adsorption capacity and the viscosity. The significant improvement of behavior at low-speeds indicates that there was an occurrence of solid-liquid phase separation in the pure paste (PP) and the MHEC decreased this tendency as the migration of liquid to the peripheral regions of the sample is larger at low speeds and when the liquid phase has a low viscosity [16, 19, 20]. The results of phase separation cited before prove this fact. In the squeeze-flow tests at 5.0 mm/s, the effect of the additive on the increase in the liquid phase viscosity was very intense. Thus, if on one hand it may have a reduced phase separation, on the other hand, it increased the viscous response of the suspension. Therefore, a higher speed meant a higher effort. Therefore, the pastes with MHEC when submitted to the tests at a high speed presented a less significant reduction in the stress levels when compared to PP.

In the squeeze-flow tests, the boundary conditions at the interfaces of the material with the plates influence the stresses on the material. The elongational deformation, which is elongation due to biaxial extension, occurs in the case of a perfect slip (zero friction), and the shear deformation is obtained when there is no slip between the plates and the material [14–17, 20]. In practice, the experiments usually show an intermediate situation with both

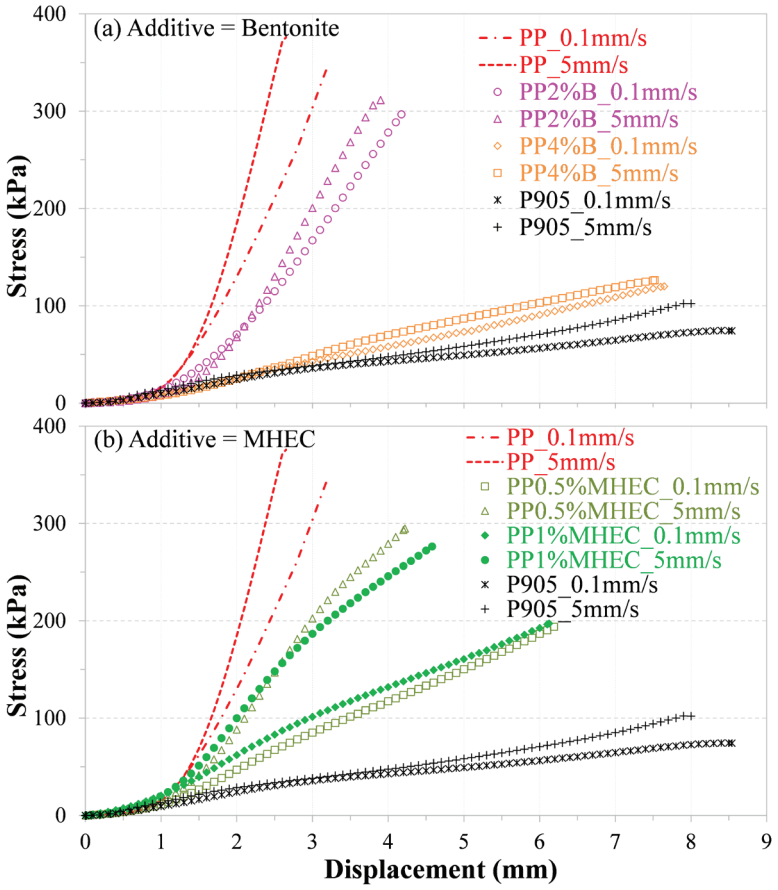

Figure 10. Squeeze flow curves of PP with and without additives tested at two different speeds of 0.1 mm/s and 5.0 mm/s; (a) with bentonite additive (b) with MHEC additive; reference curves of P905 are also shown (stress values were calculated considering the area variation for constant volume deformation of an incompressible fluid).

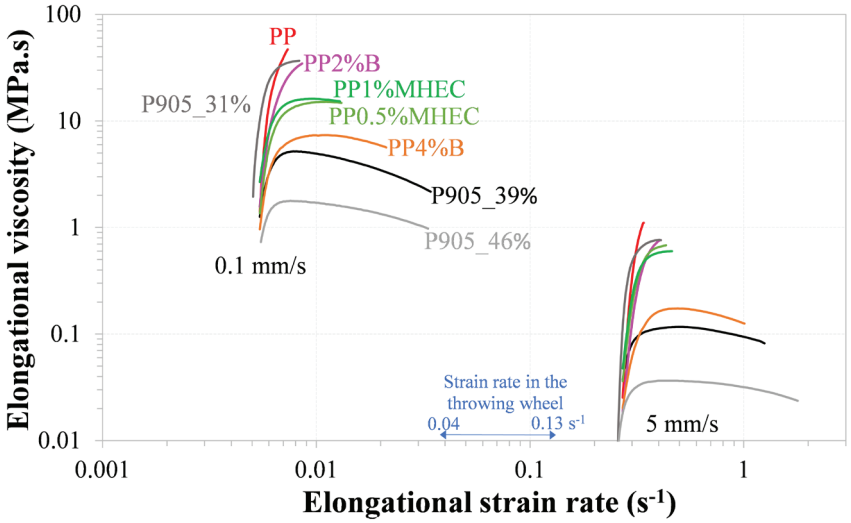

Figure 11. Elongational viscosity of the ceramics as a function of the elongational strain rate for the squeeze-flow tests at 0.1 mm/s and 5.0 mm/s.

types of deformation; however, according to the plate roughness and the lubricant characteristics of the material, one or the other type of flow may be predominant. This study employed smooth metal plates (rectified) and, therefore, it is reasonable to consider the predominant elongational deformation (or biaxial extension) [15–17]. Thus, the squeeze-flow results can be expressed in the form of elongational viscosity curves (η_B) as a function of the elongational strain rate (ε_B), which are calculated according to Eqs. 1 and 2.

$$\dot{\varepsilon}_B = \frac{\dot{\varepsilon}_H}{2} = \frac{v}{2h} \quad (1)$$

$$\eta_B = \frac{\sigma_B}{\dot{\varepsilon}_B} = \frac{F2h}{\pi r^2 v} \quad (2)$$

where (ε_H) = Henky strain rate, v = displacement speed of the top plate, and h = instantaneous sample height. The elongational viscosity (biaxial extension) η_B is the stress σ_B divided by (ε_B); where F is the normal force, and r is the instantaneous radius of the sample [16, 17]. As the constant plate displacement speed and the constant sample volume configuration were used, h and r are defined by Eq. 3 and 4, respectively, where, h_0 is the initial sample height, and R_0 is the initial sample radius.

$$h = h_0 - vt \quad (3)$$

$$r^2 = \frac{R_0^2 h_0}{h} \quad (4)$$

Fig. 11 shows the elongational viscosity curves for all the tested compositions. The elongational deformation rate varies as a function of the sample height in each individual test, and as a function of the superior plate speed. The estimated elongational strain rate for the squeeze-flow practical tests is shown in Fig. 11. The evaluation assumed the cylinder wall thickness, which was pressed between the operator´s fingers as the squeeze-flow sample height. Analyzing the results for each displacement speed, the same behavior is observed in Fig. 9 and Fig. 10. However, when comparing the pastes with good performance in the throwing wheel (P905_39% and PP 4% bentonite) to the compositions with improper behavior, especially PP with no additives, the viscosity levels vary approximately an order of magnitude. The viscosity of the latter increases intensely and continuously with the elongational strain rate within the same test (displacement speed), indicating a shear-thickening behavior, which can lead to a loss of cohesion and fractures in the material. On the contrary, the plastic pastes presented an initial increase in viscosity related with the transient conditions at the beginning of the flow, and after a remarkable transition, the viscosity fell progressively, characterizing a shear-thinning behavior.

Comparing the curves obtained at different speeds, a similar behavior is observed. However, at 5.0 mm/s, viscosity values are approximately two orders of magnitude lower than the ones with 0.1 mm/s. The stress levels in the tests are similar; however, the speed (displacement rate) is 50 times higher. Another difference is the behavior of the PP with the addition of MHEC. At 0.1 mm/s, the curves presented a viscosity plateau during the test, although at superior levels when compared to those of P905_39% and PP 4% bentonite. The curves for the tests at 5.0 mm/s, the increase of viscosity was substantial, with a slight decrease tendency in the slope in the final stages.

By definition, the yield stress is a characteristic rheological parameter of materials with a plastic behavior. In the squeeze-flow, as for any other rheological characterization technique, the yield stress is determined directly by tests controlled by stress. Through deformation rate controlled tests it is possible to estimate the yield stress using an indirect manner, by extrapolating the curves to zero rate or even identifying a transition point. The

latter has been used in the squeeze-flow tests in mortar [16], clays [12], and standard pastes such as *ballotini* concentrated in an aqueous solution of glucose [27]. However, in the present study, the curves did not present an identifiable transition point from the elastic regime to the plastic or the viscous stage, making it impossible to determine the yield stress. This situation can be linked to the constant volume configuration, the sample geometry (D/h ratio), or even the behavior of this type of material. This will be addressed in the future works.

In the squeeze-flow tests with a constant speed, the material flow is unavoidable [17], the results, like stress or elongational viscosity are still useful for understanding the behavior of the materials with the proviso that the yield stress is somehow within the calculated parameters.

An additional way to analyze the squeeze-flow results, considering elongational strain and depending on the characteristics of the material and the test, is the determination of the rheological parameters of the power law model ($\sigma = K(\dot{\gamma})^n$) for shear deformation under steady state regime [15, 17]. Eq. 5 shows the necessary force for the squeeze-flow in a constant speed of a power law type of flow. Thus, to calculate n (rheological coefficient) and K (consistency index), the logarithm is applied on both sides of Eq. 5, giving n as the slope of the linear part of the curve ln (F) vs. ln (1/h) (Eq. 6) and K from the intercept on the y-axis, C1 (Eq. 7). Fig. 12 represents the graphical procedure to determine n and K. The initial part is discarded and only the linear part of the curve (steady state) is used for the calculations.

$$F = \frac{3^{(n+1)/2} r^2 \pi K v^n}{h^n} \quad (5)$$

$$\ln(F) = C_1 + n \ln\left(\frac{1}{h}\right) \quad (6)$$

$$C_1 = \ln\left(3^{(n+1)/2} r^2 \pi K v^n\right) \quad (7)$$

The results of the parameters n and K are shown in Fig. 13 and Table 5. At 0.1 mm/s, the plot shows a direct relationship between K and n. The composition of P905 with 39% and 46% water and PP with 4% bentonite presented the lowest rheological parameters (n and K), highlighting n lower than 1, proving the pseudoplastic behavior. On the contrary, PP and PP 2% bentonite presented K values of 9 to 15 orders of magnitude higher and n values greater than 1, confirming the high shear-thickening behavior of these compositions. The increase in the bentonite content and the use of MHEC in the PP, as well as the increase in the water content in the P905 reduced both rheological parameters.

Results calculated from the tests with 5.0 mm/s are however dispersed and do not follow any trend that can be interpreted as a relationship between the parameters. The variation range of the consistency index K is significantly lower than for 0.1 mm/s (same order of magnitude) and n, however presents a wider range. The increase in the water content in P905 shows a reduction in n and K; however, it is more pronounced in K. PP showed the same level of consistency of the reference material (P905_39%), but with a much higher n value (approximately 20) when compared with that of the reference porcelain (< 1). The use of additives in

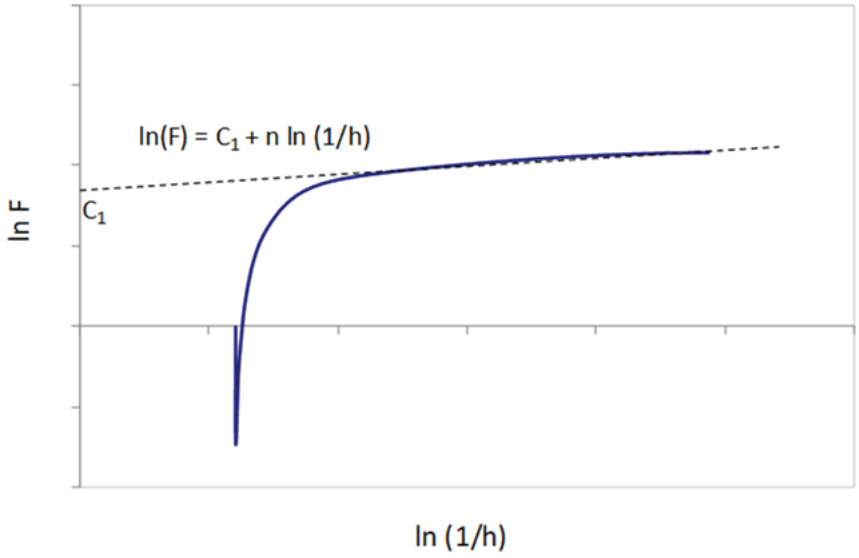

Figure 12. Plot of ln F vs. ln 1/h used for determination of steady-state shear flow Power law parameters n and K.

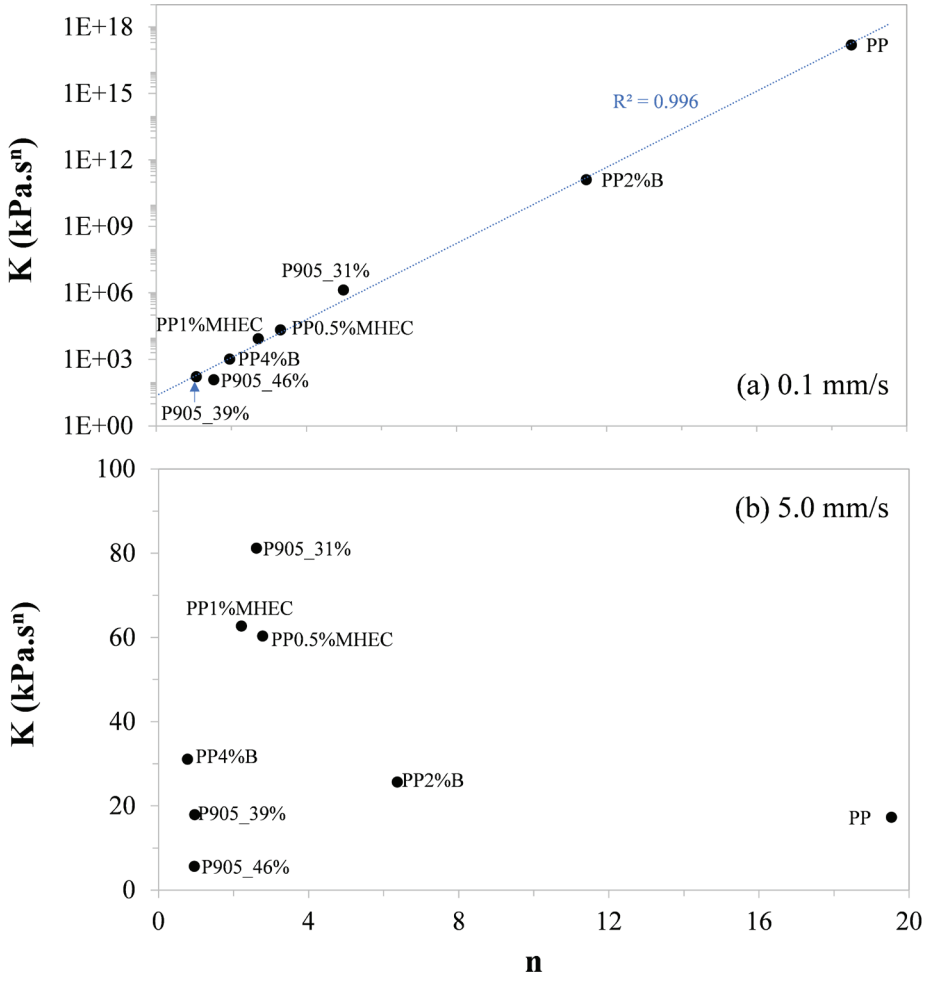

Figure 13. Power law rheological parameters n and K for a steady-state shear determined from the squeeze-flow results (a) 0.1 mm/s (b) 5.0 mm/s.

PP reduced n but increased K. The effect in n was more pronounced with 4% bentonite, while in K, an increase higher than three times can be observed.

The differences in the relation between the parameters K and n obtained at 0.1 mm/s and 5 mm/s are associated to the predominant response of each material at different velocities. During the squeeze-flow of the concentrated suspensions phase separation can occur depending on the combination of various characteristics of the material such as particle size distribution, solid concentration, viscosity of the liquid phase, and of the test such as plate roughness, geometry, and displacement speed [15, 16, 18–20]. Homogeneous flow and filtration are competing phenomena in this situation and the applied displacement rate is a key parameter, however the critical velocity that defines the flow or the filtration depends on the features of the material [19, 20]. Slower the speed, higher is the likelihood of filtration. Consequently, the particle friction acts in several pastes however probably in different extents, causing the consistency index to vary several orders of magnitude between the plastic and non-plastic ceramics and thereby affecting n significantly. On the contrary, faster the deformation, greater is the tendency to a homogeneous flow and, therefore, a viscous response tends to be predominant, with a less granular response. At 5 mms/s, K was the main varying parameter for most of the formulations, while n was very high only for the pure PP and PP2% B, which were still governed by granular frictional even at a high speed as indicated by the strain hardening profile of the stress vs. displacement curves.

The effect of the additives regarding the strain rate highlights the differences in the action mechanisms. They both have the capacity to retain water, however the MHEC acts primarily in the liquid medium [11, 26], increasing the viscosity. This change reduces or eliminates the tendency of phase separation and improves the lubrication among the particles slightly, resulting in an improvement in the material behavior especially when subjected to lower speeds. On the contrary, the lamellar particles of bentonite, besides the destabilization of the dispersion state of the system, can retain water in the inter-lamellar spaces reducing or eliminating the phase separation. In addition, they are able to orient themselves and to deform significantly due to the relative displacement among the lamellae strongly bounded by Van der Wall's forces. This contributes to a high cohesion and deformation extension, leading to an increase in plasticity. The introduction of enough amount of bentonite made the cohesion and the lubrication effects among the particles of the non-plastic materials such as the bovine bone ash and feldspar, accounting 75% of the dry composition to be reflected in the plastic behavior of the system at both the applied speeds.

Table 5 highlights the extension of the squeeze-flow curve used to determine n

Table 5. Parameters n and K; range of the displacement curve corresponding to the linear part of ln F vs. ln 1/h with a $R^2 = 0.93$ is also indicated (values for P905_39% are highlighted for reference).

Speed (mm/s)	Composition	*n*	K (kPa.s^n)	Range (mm)	Extension (mm)
0.1	P905_31%	2.5	$1.4x10^6$	1.4 – 4.0	2.6
	P905_39%	**0.53**	**$1.6x10^2$**	**2.7 – 8.4**	**5.7**
	P905_46%	0.76	$1.2x10^2$	1.5 – 8.5	7.0
	PF	9.3	$1.5x10^{17}$	1.1 – 3.2	2.1
	PP2% B	5.7	$1.3x10^{11}$	1.3 – 4.2	2.9
	PP4% B	0.98	$1.0x10^3$	2.7 – 7.6	4.9
	PP0.5% MHEC	1.7	$2.2x10^4$	2.1 – 6.2	4.1
	PP1% MHEC	1.4	$8.6x10^3$	2.1 – 6.1	4.0
5.0	P905_31%	2.6	81	1.5 – 3.9	2.4
	P905_39%	**0.96**	**18**	**1.6 – 8.0**	**6.4**
	P905_46%	0.95	5.6	1.6 – 8.6	7.0
	PP	20	17	0.5 – 2.7	2.2
	PP2% B	6.4	26	1.7 – 3.9	2.2
	PP4% B	0.77	31	3.3 – 7.5	4.2
	PP0.5% MHEC	2.8	60	2.3 – 4.2	1.9
	PP1% MHEC	2.2	63	2.1 – 4.6	2.5

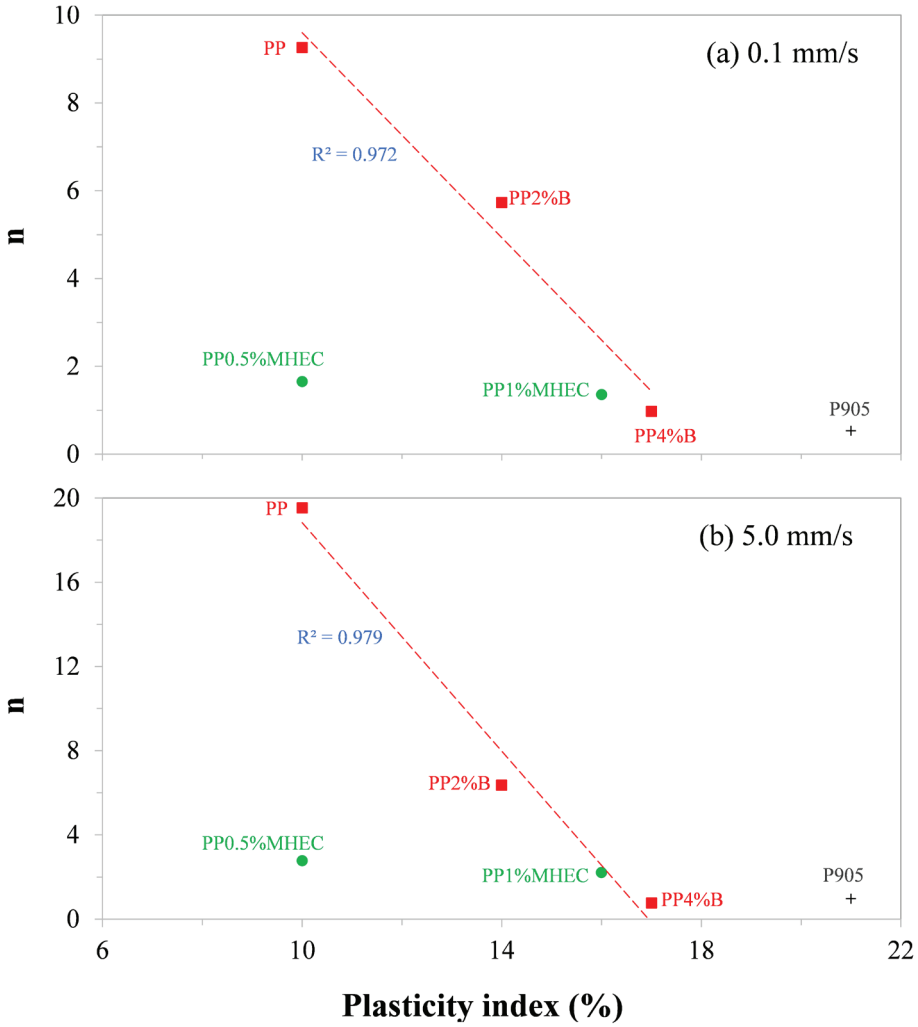

Figure 14. Results of n vs. values of Atterberg plasticity index (a) 0.1 mm/s (b) 5.0 mm/s.

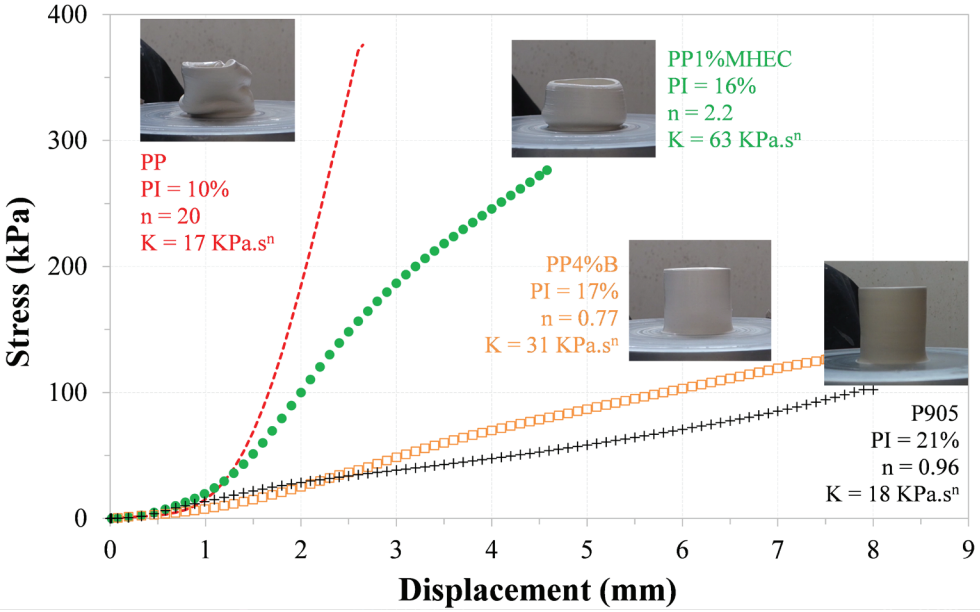

Figure 15. Comparison between the ceramics formulations; squeeze flow curves at 5.0 mm/s, PI using the Atterberg method, n and K Power law parameters and images of practical tests in the throwing wheel.

and K with a linear adjustment of $R^2 = 0.93$. This range is related to the steady state regime and presented an inverse relationship with n, suggesting in general that lower the n and greater the extension in this regime, the more plastic and suitable is the ceramic composition to be used in the throwing wheel.

Fig. 14 shows the results of the coefficient of rheological behavior n obtained by the squeeze-flow and the plasticity index using the Atterberg method. While observing the effect of bentonite on the PP paste, a linear inverse relationship between n and the plasticity index is observed. However, with MHEC, the relationship is not clear. The MHEC mechanisms have some effect on the plasticity index, however they are not specifically related with the cohesion and the plastic deformation capacity. Thus, the Atterberg method proved to be efficient to evaluate the materials with plastic characteristics. However, when additives are used or formulations are changed and there are no effects in the plasticity, the Atterberg method is insufficient to understand the phenomena.

The main results of this study are compiled in Fig. 15. It associates the performance of the ceramic pastes in the throwing wheel with the PI values, squeeze-flow curves (5.0 mm/s), and the rheological parameters. In general:

- A low PI, $n > 1$, and a high K indicate an improper behavior for the throwing wheel.
- A high PI*, $n \leq 1$, and a low K indicate an appropriate behavior for the throwing wheel.

  * A high PI does not ensure a high performance.

4. Conclusions

Ceramic pastes for shape forming in the throwing wheel were evaluated using the Atterberg method, squeeze-flow, and practical tests. A commercial porcelain (P905) adequate for the proposed processing was used as the reference and the experimental results confirmed its high practical performance, displaying its relation to a high Atterberg PI, rheological parameter $n \leq 1$ (pseudoplastic), and a low K. On the contrary, PP (50 wt% calcined bovine bones + 25 wt% feldspar + 25 wt% kaolin), with an inadequate behavior to be shaped by a throwing wheel is characterized mainly by a low PI and $n >> 1$ which implies an intense shear thickening. The use of MHEC extended the water retention capacity of PP, increased the plasticity index, reduced the phase separation, and improved the squeeze-flow behavior. However, these changes were not enough to eliminate the shear thickening behavior and the high viscosity levels, resulting in an inadequate performance during processing in the throwing wheel. The incorporation of 4% bentonite, with lamellar particles able to absorb water, align, and deform considerably in response to the flow, reduced or eliminated the phase separation and the high friction level among the particles that caused the shear thickening and the strain hardening of the pure PP composition. Both the squeeze-flow curves and the throwing wheel tests indicated the PP with 4% bentonite as the ceramic paste with the closest rheological behavior and practical performance to the P905 among the materials studied.

The squeeze-flow test proved to be an effective technique to evaluate the rheological behavior of high-consistency pastes used in the throwing wheel. The stress-displacement curves give relevant information to differentiate plastic and non-plastic pastes. The analysis of the elongational viscosity and the rheological parameters n and K in different displacement rates was able to provide detailed differences regarding the behavior of the ceramic pastes and the effect of different additives. The conclusions obtained from the squeeze-flow tests were coherent with the practical performance of the ceramics during shape forming in the throwing wheel.

Acknowledgments

The authors are grateful to the National Council for Scientific and Technological Development (CNPq) for the scholarship granted to carry out this work and FAPESP (proc. 03 / 12721-2 "Development of National Process for Bone Porcelain Manufacturing - Bone China) for the support provided to the work.

References

[1] Braganca, S.R., Bergmann, C.P.; Produção de porcelana de ossos e caracterização de suas propriedades técnicas, Cerâmica, 2006, vol.52, n.322, p.205-212.

[2] Indicadores IBGE: Estatística da Produção Pecuária. Rio de Janeiro: IBGE; [cited 2019 Oct 17]. Available from: https://biblioteca.ibge.gov.br/visualizacao/periodicos/2380/epp_2019_2tri.pdf

[3] Kara, A., Stevens, R., Characterisation of biscuit fired bone china body microstructure. Part I: XRD and SEM of crystalline phases, Journal of the European Ceramic Society, Volume 22, Issue 5, 2002, Pages 731-736.

[4] Cooper, J.J., Bone for Bone China, British Ceramic Transactions, J. 94, 4 (1995) 165.

[5] Rado, P.; An Introduction to the Technology of Pottery, 2nd Ed. The Institute of Ceramics, Pergamon Press, Oxford (1988).

[6] Dinger, D.R.; Rheology for Ceramists, 1st Ed., Morris Publishing (2002).

[7] Silva, A.R.V., Ferreira, H.C.; Esmectitas organofílicas: conceitos, estruturas, propriedades, síntese, usos industriais e produtores/fornecedores nacionais e internacionais, Revista

Eletrônica de Materiais e Processos, v.3.2 (2008) 26-35.
[8] Onikata, M.; Characteristics and Application of Bentonite. The Clay Science Society of Japan, v.46, No. 2, p. 131-138, 2007.
[9] Lagaly, G.; Principles of flow of kaolin and bentonite dispersions, Applied Clay Science, Volume 4, Issue 2, 1989, Pages 105-123.
[10] Santos, P.S.; Tecnologia de argilas aplicada às argilas brasileiras, Ed. Blücher, v.1 (1975).
[11] Pourchez, J., Peschard, A., Grosseau, P., Guyonnet, R., Guilhot, B., Vallée, F.; HPMC and HEMC influence on cement hydration, Cement and Concrete Research, 36 (2006) 288-294.
[12] Andrade, F.A., Al-Qureshi, H.A., Hotza, D.; Measuring the plasticity of clays: A review, Applied Clay Science, Volume 51, Issues 1-2, 2011, Pages 1-7.
[13] Moore, F.; Rheology of Ceramic Systems, 1st Ed.,Elsevier, cap.2 (1965).
[14] Cardoso, F.A., Pileggi, R.G., John, V.M.; Squeeze-flow aplicado a argamassas de revestimento: manual de utilização. Boletim técnico EPUSP, PCC (2010).
[15] Engmann, J., Servais, C., Burbidge, A.S.; Squeeze flow theory and applications to rheometry: A review, Journal of Non-Newtonian Fluid Mechanics, Volume 132, Issues 1-3, 2005, Pages 1-27.
[16] Cardoso, F.A., John, V.M., Pileggi, R.G.; Rheological behavior of mortars under different squeezing rates, Cement and Concrete Research, Volume 39, Issue 9, 2009, Pages 748-753.
[17] Steffe, J.F.; Rheological methods in food process engineering, Freeman Press (1996).
[18] Özkan, N., Oysu, C., Briscoe, B.J., Aydin, I.; Rheological analysis of ceramic pastes, Journal of the European Ceramic Society, Volume 19, Issue 16, 1999, Pages 2883-2891.
[19] Poitou, A., Racineux, G.; A squeezing experiment showing binder migration in concentrated suspensions, Journal of Rheology, 45 (2001) 609.
[20] Grandes, F.A., Sakano, V.K., Rego, A.C.A., Cardoso, F.A., Pileggi, R.G.; Squeeze flow coupled with dynamic pressure mapping for the rheological evaluation of cement-based mortars, Cement and Concrete Composites, Volume 92, 2018, Pages 18-35.
[21] Associação Brasileira de Normas Técnicas, ABNT NBR 15839:2010, (2010).
[22] Polidori, E.; Relationship between the atterberg limits and clay content, Soils and Foundations, v. 47, No.5 (2007), 887-896.
[23] Gouvea, D., Bernard, S., Alatrista, G.A.V., Tofolli, S.M.; Efeito da temperatura de calcinação nas propriedades de ossos bovinos para a fabricação de porcelana de ossos. Cerâmica. 2007, vol.53, n.328, pp.423-428.
[24] Gouvea, D.; Hirakata, S., Kahn, H.; Efeito da modificação da composição química na sinterização e microestrutura de porcelanas de ossos bovinos. Cerâmica. 2010, vol.56, n.340, pp.393-398.
[25] The Pottery Supply House Limited, 905 C905X Safety Data Sheet. http://www.psh.ca/MSDS/CLAY%20PSH%20905.pdf, 2017 (accessed 10 June 2019).
[26] Cappellari, M., Daubresse, A., Chaouche, M.; Influence of organic thickening admixtures on the rheological properties of mortars: Relationship with water-retention, Construction and Building Materials, Volume 38, 2013, Pages 950-961.
[27] Patel, M.J., Blackburn, S., Wilson, D.I.; Modelling of pastes as viscous soils – Lubricated squeeze flow, Powder Technology, Volume 323, 2018, Pages 250-268.